DE GRUYTER OPEN

Curved and Layer. Struct. 2015; 2:331–350

Research Article

Open Access

Achchhe Lal*, Nikhil M. Kulkarni, and B.N. Singh

Stochastic Thermal Post Buckling Response of Elastically Supported Laminated Piezoelectric Composite Plate Using Micromechanical approach

Abstract: In this paper, second order statistics of thermally induced post buckling response of elastically supported piezoelectric laminated composite plate using micromechanical approach is examined. A C^o finite element has been used for deriving eigenvalue problem using higher order shear deformation theory (HSDT) with von-Karman nonlinearity. The uncertain system properties such as material properties of fiber and matrix of composite and piezoelectric, fiber volume fraction, plate thickness, lamination angle and foundation are modeled as random variables. The temperature field considered to be uniform temperature distributions through the plate thickness. A direct iterative based nonlinear finite element method combined with mean-centered second order perturbation technique (SOPT) is used to find the mean and coefficient of variance of the post buckling temperature. The effects of volume fraction, fiber orientation, and length to thickness ratio, aspect ratios, foundation parameters, position and number of piezoelectric layers, amplitude and boundary conditions with random system properties on the critical temperature are analysed. It is found that small amount of variations of uncertain system parameters of the composite plate significantly affect the initial and post buckling temperature of laminated composite plate. The results have been validated with independent Monte Carlo simulation (MCS) and those available in literature.

Keywords: Micromechanical; Composite laminated plate; Thermal buckling; Uncertainty; Foundation; Piezoelectric; Perturbation

*Corresponding Author: Achchhe Lal: Department of Mechanical Engineering, SVNIT Surat-395007, India, E-mail: achchhelal@med.svnit.ac.in; Tel:+91-0261-2201993; Fax: +91-0261-2228394

Nikhil M. Kulkarni: Department of Mechanical Engineering, SVNIT, Surat-395007, India

B.N. Singh: Department of Aerospace Engineering, IIT, Kharagpur-721302, India

1 Introduction

The laminated composite structures made of polymer-matrix fiber reinforced composite are increasingly used in aerospace, marine, automotive, mechanical and structural engineering industries due to outstanding mechanical properties. The outstanding properties such as high strength and stiffness to weight ratio, very high fatigue characteristics, excellent corrosion resistance, tailoring capability, damage tolerance and high structural efficiency and durability makes them composite more attractive compare to metal counterparts.

Any structures are often supported by elastic foundation and occupy an important place in many structural applications from stability point of view. The elastic foundations are generally attached with spring foundation known as Winkler model and shear foundation known as Pasternak model. To represent the characteristic behavior of actual foundations, the spring foundation may not be accurate enough, and should be substituted by shear foundation to prevent transverse and lateral deformation both, and has been proved to be most reasonable from a design prospective.

The modeling and analysis of composite structures based on micro-mechanical approach is one of the very important areas of research. In micromechanical approach, interaction of constituent materials and evaluation of mechanical properties based on their relative volume are examined. The main purpose to use of micromechanical approach is to tailor the mechanical properties of composite structures in terms of strength and stiffness in particular direction to meet the particular structural requirements. In macro mechanical approach, it assumed that a perfect bonding between the fiber and matrix are existing and stress experience by each the ply is same and average mechanical properties are accounted. However, in micromechanical approach a perfect bonding between the fiber and matrix is a restriction that might well not be satisfied. Therefore individual effect of fiber and matrix will be examined.

When the structures are subjected to temperature change, thermal induced compressive stresses are developed in the constraint edges due to mismatch thermal expansion coefficients that lower the stiffness and therefore, lowering the strength and stability. Hence, thermal loading is one of the essential parameter and plays a significant role in the stability of a structure.

In the recent advancement, structures attached with piezoelectric layer at different position of fibre layers makes the structures smart by self monitoring and self controlling capabilities and opens new opportunities for future high performance structural systems.

All materials have inherent dispersions in system properties due to lack of complete control over the manufacturing, fabrication and processing techniques employed. Composite structures have more uncertainties and variability in their structural properties compared to conventional isotropic structures as a large number of parameters is associated with complex manufacturing and fabrication processes.

Plate thickness, fiber volume fraction and lamination angle are considered as important variables in structural design. Variations in the plate thickness, fiber volume fraction and lamination angle in terms of mean and variance can play an important role in the accurate prediction of the strength of the final product with satisfactory tolerances. Similarly, the effect of foundation parameters over which structures are resting is one of the areas of research. The foundation parameters are depends upon the material properties of constituents materials, and therefore they may also assume as random variables for accurate prediction of foundation behavior.

Considering the above aspects, the thickness of laminate, fiber volume fraction, lamination angle, foundation parameters and lamina micro material properties, may be modeled as basic random variables (RVs) for safe and reliable applications. Otherwise the predicted response may differ significantly from the observed values and structures may not be safe.

In common deterministic approach, these structural variables are taken to be deterministic and the variations in these variables up to certain limits are ignored, leading to approximation. Composite structures are more appropriately modeled with random system parameters where an accurate analysis is required using probabilistic approach.

Considerable research has been conducted to characterize the mechanical and thermal initial and post buckling response of structures made of composites. However, much of the published work are based on deterministic analysis and relatively little work is available on structures made of composites with random system parameters.

Considerable researches based on the deterministic analysis have been done on the initial and thermal post buckling investigations of composite plates using either classical theory of plates, first-order shear deformation theory (FSDT) and higher order shear deformation theory (HSDT) subjected to uniform or non uniform temperature distribution with temperature independent material properties [1–10]. The elaborations of important literatures related to this paper are highlighted only due to limitation of publication pages.

Very significant works on stability of plate supported by linear or nonlinear elastic foundation have been done by many researchers [11–17].

Considerable literatures are available on buckling on plate and/or shell attached with smart materials between the layers of different fibers [18–22].

However, limited numbers of literatures are available for the analysis of plate using the micromechanical approaches based on degradation of material properties [23–27].

Very limited literatures are available on the initial and post thermo mechanical buckling of plates, shells and beam supported with and without elastic foundation with system randomness. In this direction, Graham and Siragy [28] studied the random buckling loads of beams and plates with stochastically varying material and geometrical properties using concept of variability response function. The elastic modulus, moment of inertia and thickness are assumed to be described by homogeneous stochastic fields. Onkar et al. [29] have investigated the generalized buckling analysis of laminated plate with random material properties using stochastic finite element method using generalized layer wise theory. Verma and Singh [30] evacuated the thermal buckling of laminated composite plate using HSDT with C^o continuity. They examined the effect of random material and geometrical properties on the buckling temperature of the plate using first order perturbation method (FOPT).

Lal et al. [31] used the first order perturbation method to examine the statistics of thermal buckling of laminated composite plate through C^o finite element method via HSDT. Lal et al. [32] examined the effect of random material properties on the thermal buckling of laminated composite plate subjected to temperature dependent and independent thermo-material properties. They used C^o finite element method in conjunction with FOPT via HSDT to find the mean and standard deviation of thermal buckling temperature. Singh and Jibumon [33] evaluated the thermal buckling of conical panels embedded with and without

piezoelectric layers with random material properties. They used FOPT to handle the randomness in material properties. Kumar et al. [34] evaluated the hygrothermoelastic induced buckling response of laminated composite plate using macro and micromechanical approach. They used C^o FEM combined with FOPT through HSDT to solve the random governing equation.

The contribution of this paper is to evaluate the mean and coefficient of variation of thermal post buckling response of elastically supported piezoelectric laminated composite plate with random system properties using SOPT.

However, to the best knowledge of author's knowledge, very little literature covering the thermal post buckling behavior of piezoelectric laminated plate resting on elastic foundation subjected to random system properties using SOPT via micromechanical approach. This is the problem studied in the present paper. The proposed outlined probabilistic procedure would be valid for system properties with small random dispersion compared to their mean values. Fortunately, most of the engineering materials such as composite fall in this category.

2 Formulation

2.1 Geometrical consideration of piezolaminated elastically supported plate

The piezoelectric multilayered composite plate supported with two parameter Pasternak foundation consisting of spring layer and shear layer with foundation stiffnesses K_1 and K_2, respectively having length a, width b, thickness h located in the three dimensional Cartesian coordinate system (x, y, z) is shown in Fig. 1, where x and y are in the axial and tangential directions of plate and z is normal to the mid surface of plate, respectively. The plate consists N plies in which, the upper ply and lower ply are respectively, integrated piezoelectric actuator and sensor layers of thickness h_a and h_s bonded on the composite laminates. It is assumed that a perfect bonding exists between the fibers and the matrix so that no slippage can occurs at the interface. The fibers are assumed to be uniform in properties and diameter continues and parallel throughout the composite. It is also assumed that the composite behaves like heterogeneous composite material and the effect of the constituent's materials (i.e., matrix and fiber) are detected separately.
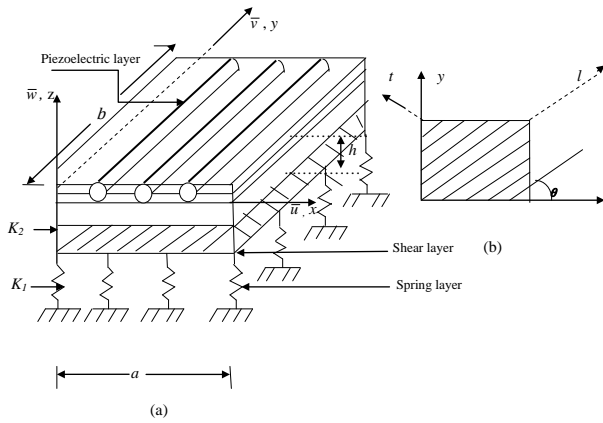

Figure 1: Geometry of piezolaminated laminated composite plate resting on elastic foundation.

It is also assumed that plate supported with elastic foundation excluding any separation takes place between the plate and the supporting foundation follows the two-parameters model known as Pasternak foundation model and expressed as [11, 12]

$$P = K_1 w - K_2 \left[\frac{\partial^2 w}{\partial x^2} + \frac{\partial^2 w}{\partial y^2} \right] \qquad (1)$$

Where P, K_1 and K_2 and w are the foundation reaction per unit area, normal (spring) and shear stiffness of the foundations and transverse deflection, respectively. The above model is simply known as Winkler type when K_2 is considered as zero.

2.2 Displacement model

In the present work, the assumed displacement field is based on HSDT given by Reddy [35]. The Displacement fields $(\overline{u}, \ \overline{v}, \ \overline{w})$ at any point along (x, y, z) directions for a composite plate can be expressed as

$$\begin{aligned}
\overline{u} &= u + z\psi_x - z^3 4/3h^2(\psi_x + \partial w/\partial x) = u + f_1(z)\psi_x \\
&\quad + f_2(z)\partial w/\partial x, \\
\overline{v} &= v + z\psi_y - z^3 4/3h^2(\psi_y + \partial w/\partial y) = v + f_1(z)\psi_y \\
&\quad + f_2(z)\partial w/\partial y, \\
\overline{w} &= w, \qquad\qquad\qquad\qquad\qquad\qquad\qquad\qquad (2)
\end{aligned}$$

Where u, v, w are the corresponding displacements of a point on the middle surface, and ψ_x and ψ_y are the rotations at z=0 of normal to the mid-surface with respect to the x and y axes, respectively. The $f_1(z)$ and $f_2(z)$ are represented as,

$$f_1(z) = C_1 z - C_2 z^3 \ And f_2(z) = -C_4 z^3 \qquad (3)$$

Where C_1, C_2 and C_4 are constants. The values of these constants are, $C_1 = 1$, $C_2 = C_4 = 4/3h^2$.

The displacement field in Eq. 1, for in-plane displacement $\bar{u}$ and $\bar{v}$ involve the derivatives of out of plane displacement w. As a result of this, second order derivatives would be present in the strain vector; therefore C^1 continuity occurs in the analysis. The solution of finite element problem using C^1 continuity requires more computational cost with extra complexity. To avoid this problem, two additional variables have been included in the displacement field as $\theta_x = \partial w/\partial x$ and $\theta_y = \partial w/\partial y$ to make C^o continuity in order to satisfy all constraints. Thus five DOFs with C^1 continuity in Eq. 2 can be increased to 7 DOFs with C^0 continuity due to conformity with HSDT.

This is circumvented by expressing the displacement field in the following form [21, 22, 31–34]

$$\bar{u} = u + f_1(z)\psi_x + f_2(z)\theta_x; \quad \bar{v} = v + f_1(z)\psi_y + f_2(z)\theta_y; \quad \bar{w} = w \tag{4}$$

The displacement field vector $\{q\}$ for the modified C^0 continuous model is expressed as

$$q = \begin{pmatrix} u & v & w & \theta_2 & \theta_1 & \phi_2 & \phi_1 \end{pmatrix}^T \tag{5}$$

2.3 Strain displacement relations

The strain-displacement relations are obtained by using large deformation theory with von-Karman nonlinearity. The total strain vectors associated with displacement for lamina layers can be expressed as

$$\{\varepsilon\} = \{\varepsilon_l\} + \{\varepsilon_{nl}\} - \{\varepsilon_t\} - \{\varepsilon_p\} \tag{6}$$

The linear strain tensor $\{\varepsilon_l\}$ based on HSDT can be written as

$$\{\varepsilon_l\} = [T]\{\bar{\varepsilon}_l\} \tag{7}$$

Where, T is the function of Z and unit step vector defined in Appendix A.1 and ε_{kl}^L is reference plain linear strain tensor defined as

$$\{\bar{\varepsilon}_l\} = \left\{ \varepsilon_1^0 \ \varepsilon_2^0 \ \varepsilon_6^0 \ k_1^0 \ k_2^0 \ k_6^0 \ k_1^2 \ k_2^2 \ k_6^2 \ \varepsilon_4^0 \ \varepsilon_5^0 \ k_4^2 \ k_5^2 \right\}^T \tag{8}$$

From Eq. 5, Eq. 8 can be written as

$$\{\overline{\varepsilon_l}\} = [L]\{q\} \tag{8a}$$

Assuming that the strains are much smaller than the rotations (in the von-Karman sense), one can rewrite nonlinear strain vector $\{\varepsilon_{nl}\}$ as [31–34]

$$\{\varepsilon_{nl}\} = \frac{1}{2}[A]\{\phi\} \tag{9}$$

where $[A] = \frac{1}{2}\begin{bmatrix} w,_x & 0 & w,_y & 0 & 0 \\ 0 & w,_x & w,_y & 0 & 0 \end{bmatrix}^T$

and $\phi = \frac{1}{2}\begin{bmatrix} w,_x \\ w,_y \end{bmatrix}$ \hfill (10)

here (,) denotes partial differential.

The thermal strain vector $\{\varepsilon_t\}$ can be represented as

$$\{\varepsilon_t\} = \left\{ \alpha_1 \Delta T \ \ \alpha_2 \Delta T \ \ \alpha_{12}\Delta T \ \ 0 \ \ 0 \right\}^T \tag{11}$$

Where α_1, α_2 and α_{12} are thermal expansion coefficients along the principal and shear directions, respectively. ΔT is the change in temperature from reference temperature in the plate subjected with uniform temperature which can be defined as $\Delta T = T - T_0$. Where, T_0 and T are the uniform temperature at room temperature and at a given temperature, respectively. For the generated results in tables the values of T_0 and C_0 are taken as $21°C$ and $C_0 = 0\%$.

The piezoelectric strain vector $\{\bar{\varepsilon}^P\}$ can be represented as

$$\{E\} = \left\{ E_x \ \ E_y \ \ E_z \right\} = [T_\phi]\{E^{(0)}\} \tag{12}$$

Where $[T_\Phi]$ and $[E]$ is the electric field potential operator and electric field vector, respectively and defined in Appendix A.2.

2.4 Micromechanical approach

The effective materials properties of the fiber reinforce composite at given temperature are evaluated using micromechanical model. Since, the effect of induced temperature is dominant in matrix material. The degradation of the fiber reinforced composite material properties is estimated by degrading the matrix property only. The matrix mechanical property retention ratio can be expressed as 24

$$F_m = \left[\frac{T_{gw} - T}{T_{g0} - T_0} \right]^{\frac{1}{2}} \tag{13}$$

where $T = T_0 + \Delta T$ and T is the temperature at which material property is to be predicted; The parameters T_{gw} and T_{go} are glass transition temperature for wet and reference dry conditions, respectively. The glass transition temperature for wet material can be determined as 23, 24, 25, 26, 27

$$T_{gw} = \left(0.005C^2 - 0.10C + 1.0 \right) T_{g0} \tag{14}$$

Where $C = C_0$ is the weight percent of moisture in the matrix material. $C_0 = 0$ weight percent and C is the increase in moisture content. In the present case it is considered

as zero. The elastic constants using micromechanical approach are obtained from the following equations as written as 25, 27, 38-39

$$E_{11} = E_{f1}V_f + F_mE_mV_m \qquad (15a)$$

$$E_{22} = \left(1 - \sqrt{V_f}\right)F_mE_m + \frac{F_mE_m\sqrt{V_f}}{1 - \sqrt{V_f}\left(1 - \frac{F_mE_m}{E_{f2}}\right)} \qquad (15b)$$

$$G_{12} = \left(1 - \sqrt{V_f}\right)F_mG_m + \frac{F_mG_m\sqrt{V_f}}{1 - \sqrt{V_f}\left(1 - \frac{F_mG_m}{G_{f12}}\right)} \qquad (15c)$$

$$\nu_{12} = \nu_{f12}V_f + \nu_mV_m \qquad (15d)$$

Where "V" is the volume fraction and subscripts "f" and "m" are used for fiber and matrix, respectively. The effect of increased temperature and moisture concentration on the coefficients of thermal expansion (α) is opposite from the corresponding effect on strength and stiffness. The matrix thermal property retention ratio is approximated as

$$F_h = \frac{1}{F_m} \qquad (16)$$

The coefficients of thermal expansion using micromechanical approach are expressed as [27, 38]

$$\alpha_{11} = \frac{E_{f1}V_f\alpha_{f1} + F_mE_mV_mF_h\alpha_m}{E_{f1}V_f + F_mE_mV_m} \qquad (17)$$

$$\alpha_{22} = \left(1 + \nu_{f12}\right)V_f\alpha_{f2} + (1 + \nu_m)V_mF_h\alpha_m - \nu_{12}\alpha_{11} \qquad (18)$$

2.5 Constitutive equation

The constitutive law of thermo-piezo-elastic constitutive relationship for material under consideration relates the stresses with strains in plan-stress state for the kth orthotropic lamina is given as [33]

$$[\sigma] = [Q]\{\varepsilon\} - [e]\{E\} \qquad (19)$$

Where [Q] is the constitutive elastic stiffness matrix defined in Appendix A.3

Where [e] is defined as piezoelectric constant and expressed by

$$[e] = \begin{bmatrix} 0 & 0 & 0 & e_{14} & e_{15} \\ 0 & 0 & 0 & e_{24} & e_{25} \\ e_{31} & e_{32} & e_{36} & 0 & 0 \end{bmatrix}^T \qquad (20)$$

Here [E] is the electric field vector defined by

$$\{E\} = \begin{bmatrix} E_x & E_y & E_z \end{bmatrix}^T = \begin{bmatrix} -\frac{\partial\phi}{\partial x} & -\frac{\partial\phi}{\partial y} & -\frac{\partial\phi}{\partial z} \end{bmatrix}^T \qquad (21)$$

Where φ is electric potential and defined in Appendix A-4.

2.6 Strain energy of the piezolaminated composite plates

The elastic strain energy of a piezoelectric laminated composite plate is expressed as

$$U = \frac{1}{2}\int_V \{\varepsilon\}^T\{\sigma\}\,dV - \frac{1}{2}\int_V \{E\}^T\{D\}\,dV \qquad (22)$$

The parameter [D] is the electric field displacement and defined as the elastic strain energy becomes

$$\{D\} = [e]^T\{\varepsilon\} + [k]\{E\} \qquad (23)$$

Where [k] is the dielectric constant matrix and defined in appendix A.5.

Substituting Eq. 19, 23 and 39 in Eq. 22, Eq. 22 becomes

$$U = \frac{1}{2}\int_v \left(\varepsilon^T\left[\overline{Q}\varepsilon - eE\right]\right.$$
$$\left. -E^T\left[e^T\varepsilon + kE\right]\right)dV. \qquad (24)$$

Substituting Eq. 8 in Eq. 24 once can be written as

$$U = \frac{1}{2}\int_v \left((\varepsilon_l + \varepsilon_{nl})^T\left[\overline{Q}(\varepsilon_l + \varepsilon_{nl}) - eE\right]\right.$$
$$\left. -E^T\left[e^T(\varepsilon_l + \varepsilon_{nl}) + kE\right]\right)dV \qquad (25)$$

Using Eq. 25, linear potential energy can be written as

$$U_l = \frac{1}{2}\int_V \left(\varepsilon_l^T\left[\overline{Q}\varepsilon_l - eE\right] - E^T\left[e^T\varepsilon_l + kE\right]\right)dV \qquad (26)$$

Substituting Eq. 8a and 11 in Eq. 26, Eq. 26 can be rewritten as

$$U_L = \frac{1}{2}\int_A \left(q^TL^TDLq - q^TL^TD_1L_\phi\phi - \phi^TL_\phi^TD_1^TLq\right.$$
$$\left. -\phi^TL_\phi^TD_2L_\phi\phi\right)dA \qquad (27)$$

Where D, D_1 and D_2, are the elastic stiffness matrix of composite and piezoelectric material, respectively and defined in Appendix **A. 6(a-c)**.

Using Eq. 25, after substituting Eq. 8a and 9, the nonlinear potential energy of piezoelectric composite plate is written as

$$U_{nl} = \frac{1}{2}\int_A \left(q^TL^TD_3A\phi + A^T\phi^TD_4qL + A^T\phi^TD_5A\phi\varphi\right.$$
$$\left. - A^T\phi^TD_6L_\varphi - L_\varphi^T\varphi_\varphi^TD_7A\phi\right)dA \qquad (28)$$

Where [D_3], [D_4], [D_5] are the nonlinear elastic matrix and [D_6], and [D_7] are the piezoelectric stiffness matrix, respectively and defined in Appendix A.7.

2.7 Strain energy due to elastic foundation

Using Eq. 1, the strain energy due to elastic foundation using two parameter Pasternak elastic foundation having shear deformable layer can be written as [31–33]

$$U_f = \frac{1}{2} \int_A \left[K_1 (w)^2 + K_2 \left\{ (w,_x)^2 + (w,_y)^2 \right\} \right] dA$$

$$= \frac{1}{2} \int_A \left\{ \begin{matrix} w \\ w,_x \\ w,_y \end{matrix} \right\}^T \left[\begin{matrix} K_1 & 0 & 0 \\ 0 & K_2 & 0 \\ 0 & 0 & K_2 \end{matrix} \right] \left\{ \begin{matrix} w \\ w,_x \\ w,_y \end{matrix} \right\} dA$$

(29)

Eq. 29 can be rewritten as

$$U_f = \frac{1}{2} \int_A \frac{1}{2} \varepsilon_f^T D_f \varepsilon_f dA \tag{30}$$

Where $\varepsilon_f = L_f w$ with $L_f = \left[\begin{matrix} 0 & 0 & 1 & 0 & 0 & 0 & 0 \\ 0 & 0 & \partial,_x & 0 & 0 & 0 & 0 \\ 0 & 0 & \partial,_y & 0 & 0 & 0 & 0 \end{matrix} \right]$

and $D_f = \left[\begin{matrix} K_1 & 0 & 0 \\ 0 & K_2 & 0 \\ 0 & 0 & K_2 \end{matrix} \right]$

2.8 Potential energy

The potential of thermal stresses are given by 31, 32, 33

$$V = \frac{1}{2} \int_A \left[N_x (w,_x)^2 + N_y (w,_y)^2 + 2N_{xy} (w,_x) (w,_y) \right] dA$$

(31)

$$V = \frac{1}{2} \int_A \left\{ \begin{matrix} w,_x \\ w,_y \end{matrix} \right\} \left[\begin{matrix} N_1 & N_{12} \\ N_{12} & N_2 \end{matrix} \right] \left\{ \begin{matrix} w,_x \\ w,_y \end{matrix} \right\}^T dA, \quad (32)$$

Where, N_x, N_y, and N_{xy} are in plane thermal internal loads.

2.9 Finite element model

In general, a closed form solution is difficult to obtain for buckling problems for complex boundary conditions and shapes. Therefore, FEM is the one of powerful tool used for finding an approximate solution of the problem. The displacement field vector can be written in terms of shape functions as [31–34]

Displacement vector $\{q\}$ in Eq. 5 and Eq. 21 can be written in terms of shape functions as

$$\{q\} = \sum_{i=1}^{NN} [N_i] \{q_i\}, \text{ and } \{\varphi\} = \sum_{i=1}^{NN} [N_{\varphi i}] \{\varphi_i\}, \quad (33)$$

here i represent node number and N_i is shape function at i^{th} node.

For an element, displacement field vector, and electric potential vector can be written as

$$\{q\}^{(e)} = [N_i]^{(e)} \{q\}^{(e)} \text{ and } \{\phi\}^{(e)} = \left[N_\phi \right]^{(e)} \{q_\phi\}^{(e)} \quad (34)$$

Substituting Eq. 34 in Eq. 27, and summed over all elements using finite element model Eq. 33, Eq. 27 linear strain energy of the piezolaminated plate can be rewritten as

$$U_l^{(e)} = \sum_{i=1}^{NE} \left(q^{(e)T} K^{(e)} q^{(e)} - q^{(e)T} K_1^{(e)} q_\phi^{(e)} - q_\phi^{(e)T} K_1^{(e)T} q^{(e)} \right.$$
$$\left. - q_\phi^{(e)T} K_2^{(e)} q_\phi^{(e)} - q^{(e)T} F_t^{(e)} \right)$$

(35)

Where

$$K^{(e)} = \frac{1}{2} \int_{A^{(e)}} B^{(e)T} D B^{(e)} dA, K_1^{(e)} = \frac{1}{2} \int_{A^{(e)}} B^{(e)T} D_1 B_\phi^{(e)} dA,$$

$$\text{and } K_2^{(e)} = \frac{1}{2} \int_{A^{(e)}} B_\phi^{(e)T} D_2 B_\phi^{(e)} dA, \tag{36}$$

Here $K^{(e)}$, $K_1^{(e)}$ and $K_2^{(e)}$ are the element bending stiffness matrix, coupling matrix and dielectric matrix, respectively. The strain displacement matrix $[B]$ for plate and piezoelectric $[B_g]$ can be written as

$$[B]^{(e)} = [L] [N_i]^{(e)}, \text{ and } [B_\varphi]^{(e)} = [L_\varphi] [N_\varphi]^{(e)}. \quad (37a)$$

$$\text{with } [B]^{(e)} = \left[\begin{matrix} B_1 & B_2 & B_3 & \cdot & \cdot & \cdot & B_{NN} \end{matrix} \right]$$

$$\text{and} [B_i] = [L]N_i . i = 1, 2, 3, \dots NN \tag{37b}$$

The element thermal load vector can be expressed as

$$F_t^e = \int_\Omega \left[\left[[B_{ti}]^T \{N_t\} + [B_{b1i}]^T \{M_t\} + [B_{b2i}]^T \{P_t\} \right] \right] dA.$$

(38)

Where $\{N_t\}$, $\{M_t\}$ and $\{P_t\}$ are thermal resultants per unit width and defined in Appendix A.8.

Similarly, using Eq. 28 and Eq. 33, the nonlinear strain energy for piezolaminated plate after summing over the entire element using finite element analysis can be rewritten as

$$U_{nl}^{(e)} = \sum_{i=1}^{NE} (\{q^{(e)}\}^T k_1^{(e)} \{q^{(e)}\} + \{q^{(e)}\}^T k_2^{(e)} \{q^{(e)}\} + \{q^{(e)}\}^T k_3^{(e)} \{q^{(e)}\}$$

$$- \{q^{(e)}\}^T k_4^{(e)} \{q_\phi^{(e)}\} - \{q_\phi^{(e)}\}^T k_5^{(e)} \{q^{(e)}\}) \tag{39}$$

where

$$k_1^{(e)} = \frac{1}{2} \int_{A^e} B^{(e)T} D_3 \{A^{(e)}\} \{G^{(e)}\} dx dy,$$

$$k_2^{(e)} = \frac{1}{2} \int_{A^e} \{G^{(e)}\}^T \{A^e\}^T D_4 \{B^{(e)}\} dx dy$$

and

$$k_3^{(e)} = \frac{1}{2} \int_{A^e} \{G^{(e)}\}^T \{A^{(e)}\}^T D_5 \{A^{(e)}\} \{G^{(e)}\} dx dy$$

are the element bending stiffness matrix and

$$k_4^{(e)} = \frac{1}{2} \int_{A^e} \{G^{(e)}\}^T \{A^{(e)}\}^T D_6 \{B_\phi\} dx dy$$

and

$$k_5^{(e)} = \frac{1}{2} \int_{A^e} \{B_\phi^{(e)}\}^T D_7 \{A^{(e)}\} \{G^{(e)}\} dx dy$$

are the coupling matrix, respectively.

Similarly, strain energy due to foundation after summing over all the element using Eq. 33, Eq. 30 can be rewritten as

$$U_f^{(e)} = \sum_{i=1}^{NE} \left\{q^{(e)}\right\}^T K_f^{(e)} \left\{q^{(e)}\right\} \tag{40}$$

where $K_f^{(e)} = \frac{1}{2} \int_{A^{(e)}} B_f^{(e)T} D_f B_f^{(e)} dA$, is the foundation stiffness matrix and $[B_f]$ is the strain displacement matrix due to foundation and defined as

$$\left[B_f\right]^{(e)} = \left[L_f\right] [N]^{(e)} \tag{41}$$

Using finite element model as Eq. 33, potential of work done due to thermal loading as given Eq. 32 can also be written as

$$V^{(e)} = \sum_{i=1}^{NE} \lambda \left\{q^{(e)}\right\}^T K_g^{(e)} \left\{q^{(e)}\right\} \tag{42}$$

Where λ and $[K_g]^{(e)}$ are the defined as thermal buckling load and elemental geometric stiffness matrix, respectively. The value of $[K_g]$ is defined in Appendix A.10.

Adopting numerical integration, the element bending stiffness matrix consist of linear and nonlinear, coupling matrix, dielectric stiffness matrix, foundation stiffness matrix and geometric stiffness matrix can be obtain by transforming expression in (x, y) coordinate system to natural coordinate system (ξ, η) using Gauss quadrature.

The total potential energy $\prod$ can be expressed as

$$\prod = U_l + U_{nl} + U_f + V \tag{43}$$

Substituting Eq. 35, Eq. 39, Eq. 40 and Eq. 42 in Eq. 43, Eq. 43 can be rewritten as

$$\begin{bmatrix} \lambda K_g & 0 \\ 0 & 0 \end{bmatrix} \left\{ \begin{array}{c} q \\ \phi \end{array} \right\} + \begin{bmatrix} K_f & 0 \\ 0 & 0 \end{bmatrix} \left\{ \begin{array}{c} q \\ \phi \end{array} \right\}$$

$$+ \begin{bmatrix} K & K_1 \\ K_1^T & K_2 \end{bmatrix} \left\{ \begin{array}{c} q \\ \phi \end{array} \right\} = F_t, \tag{44}$$

3 Governing equation

The governing equation for thermal buckling of laminated composite plate can be derived using Variational principle, which is generalization of the principle of virtual displacement.

For the displacement field of prebuckling, the first variation of total potential energy (Π) must be zero. Following this once obtains by using Eq. 44 [30–34]

$$\left[K^\star\right] \{q\} = [F_t] \tag{45}$$

where

$$K^\star = K_q - K_{q\_phi} K_{phi}^{-1} K_{q\_phi}^T + K_f \tag{46}$$

here

$$K_q = \sum_{e=1}^{NE} (K^{(e)} + K_1^{(e)} + K_2^{(e)}),$$

$$K_{q\_phi} = \sum_{e=1}^{NE} (K1^{(e)} + K_4^{(e)}),$$

$$K_{phi} = \sum_{e=1}^{NE} K_2^{(e)},$$

$$F_t = \sum_{e=1}^{NE} F_t^{(e)}$$

and

$$K_f = \sum_{e=1}^{NE} K_f^{(e)}.$$

The parameters K_q, K_{q_phi}, K_1^T, K_{phi} and $F_t^{(e)}$ are the global elastic stiffness matrix, coupling matrix between elastic mechanical and electrical effect, dielectric stiffness matrix, force vector and foundation stiffness matrix, respectively.

For the critical buckling temperature state corresponding to the neutral equilibrium condition, the second variation of total potential energy Π must be zero and the following standard eigenvalues problems is obtained [30]

$$\left| \left[K^\star\right] + \lambda [K_g] \right| = 0 \tag{47}$$

λ The product of and the initial guessed valve ΔT is the critical buckling temperature T_{cr}. Since the matrix $\left[K^\star\right]$ and $[K_g]$ are random in nature involving uncertain material and geometric properties. Therefore, the eigenvalues and eigenvectors also become random in nature. Eq. 47 by assuming random governing equation cannot be solve using conventional (deterministic) eigenvalue problem without changing the nature of the problem. Eq. 47 with indom system properties can be solve using probabilistic approach.

Among the given different probabilistic approach, perturbation method and Monte Carlo simulation are mostly used [36, 37]. However, perturbation approach based on first and second order Taylor series expansion relies on low order of polynomial. As the coefficient of variation becomes large, this method becomes inaccurate. Although, using this method, randomness in system properties up to 20% and their effect on response give satisfactory results [36].

The nonlinear eigenvalue problem as given in Eq. 47 can be solved by employing a direct iterative method in conjunction with second order perturbation technique by assuming the random change in the eigenvector during iteration does not much affect the nonlinear stiffness matrix. The solution procedure for solution of nonlinear random governing equation using direct iterative procedure in conjunction with stochastic finite element method (DISFEM) is highlighted by the corresponding authors in literatures of [31, 32].

4 Solution Technique

4.1 Second order perturbation technique (SOPT)

In the given Eq. 47, the operating random system variables can be expended using Taylor series expansion about the mean values of random variables up to second order without loss of any generality as [36, 37]

$$\left[K^\star\right] = \left[K_0^\star\right] + \sum_{i=1}^{N} \left[K_i^{\star I}\right] \alpha_i + \frac{1}{2} \sum_{i=1}^{N} \sum_{j=1}^{N} \left[K_{ij}^{\star II}\right] \alpha_i \alpha_j$$

$$\left[K_g^\star\right] = \left[K_{g0}\right] + \sum_{i=1}^{N} \left[K_g^{\star I}\right] \alpha_i + \frac{1}{2} \sum_{i=1}^{N} \sum_{j=1}^{N} \left[K_{gij}^{II}\right] \alpha_i \alpha_j \quad (48a)$$

$$\lambda_i = \lambda_{0i} + \sum_{i=1}^{N} \lambda_i^{I} \alpha_i + \frac{1}{2} \sum_{i=1}^{N} \sum_{j=1}^{N} \lambda_{ij}^{II} \alpha_i \alpha_j$$

and

$$\{q_i\} = \{q_{0i}\} + \sum_{i=1}^{N} \left\{q_i^{\star I}\right\} \alpha_i + \frac{1}{2} \sum_{i=1}^{N} \sum_{j=1}^{N} \left\{q_{ij}^{\star II}\right\} \alpha_i \alpha_j \quad (48b)$$

where $[K_0]$, $\left[K_{g0}\right]$, λ_0 and $\{q_0\}$ are the mean deterministic values of respective tensor. The parameter α_{ij} $(i, j = 1, \ 2)$ is statistically independent random variables.

The symbol $()_i^{\star I}$ and $()_{ij}^{\star II}$ represent the first and second order derivatives evaluated at $\alpha = 0$, for example,

$$K_i^{\star I} = \left.\frac{\partial K}{\partial \alpha_i}\right|_{\alpha=0}, \quad K_{ij}^{\star II} = \left.\frac{\partial^2 K}{\partial \alpha_i \partial \alpha_j}\right|_{\alpha=0} \quad (49)$$

By using random variables obtained Eq. 48 in Eq. 47 and after simplification following equations are obtained

$$\left[K_0^\star\right] \{q_{0i}\} = \lambda_{0i} \left[K_{g0}\right] \{q_{0i}\} \quad \dots \text{ zeroth order} \quad (50)$$

$$\left(\left[K_0^\star\right] - \lambda_{0i} \left[K_{g0}\right]\right) \left\{q_i^{\star I}\right\}$$
$$= -\left(\left[K_i^{\star I}\right] - \lambda_{0i} \left[K_{gi}^{\star I}\right] - \lambda_i^{\star I} \left[K_{g0}\right]\right) \{q_{0i}\} \quad \dots \text{ first order}$$
$$(51)$$

$$[K_0] \left\{q_i^{\star II}\right\} + \left[K_i^{\star I}\right] \left\{q_i^{\star I}\right\} + \left[K_{ij}^{\star II}\right] \{q_{0i}\} = \lambda_{i0} \left[K_{g0}\right] \left\{q_i^{\star II}\right\}$$
$$+ \lambda_{0i} \left[K_g^{\star I}\right] \left\{q_i^{\star II}\right\} + \lambda_{0i} \left[K_g^{\star II}\right] \{q_{0i}\} + \lambda_i^{\star I} \left[K_{g0}\right] \left\{q_i^{\star I}\right\}$$
$$+ \lambda_i^{\star I} \left[K_g^{\star I}\right] \{q_{0i}\} + \lambda_i^{\star II} \left[K_{g0}\right] \{q_{0i}\} \text{ second order} \quad (52)$$

Obviously, Eq. 50 is a deterministic equation relating to mean quantities. The mean eigenvalues and corresponding eigenvectors can be determined by conventional eigen solution procedures. Eq. 51 and Eq. 52 being first order and second order represent their random counterpart and solution of these equation gives the statistics in terms of mean and standard deviation of the buckling temperature. The solution of these equations requires probabilistic analysis. In this procedure, the eigenvector are normalized using orthogonality conditions to make it complete orthonormal set. These normalized eigenvector is used to evaluate the covariance of buckling temperature.

The variance values for first order and second order of stress are written as [36, 37]

$$Var^I [\lambda, \lambda] \approx \sum_{i=1}^{N} \sum_{j=1}^{N} \left\{\lambda_i^{\star I}\right\} \left(\left\{\lambda_j^{\star I}\right\}\right)^T COV \left[\alpha_i, \alpha_j\right] \quad (53)$$

$$Var^{II} [\lambda, \lambda] = Var^I [\lambda, \lambda]$$
$$+ \frac{1}{4} \sum_{i=1}^{N} \sum_{j=1}^{N} \sum_{k=1}^{N} \sum_{l=1}^{N} \lambda_{ij}^{\star II} \left(\lambda_{kl}^{\star II}\right)^T \left(E \left[\alpha_i \alpha_l\right] E \left[\alpha_j \alpha_k\right]\right.$$
$$\left. + E \left[\alpha_i \alpha_k\right] E \left[\alpha_j \alpha_l\right]\right) \quad (54)$$

The $COV \left[\alpha_i, \alpha_j\right]$ in Eq. 53 can be evaluated in terms of correlation coefficients ρ_{ij} and expressed as

$$Cov \left[\{\lambda\}, \{\lambda\}\right] = \sum_{i=1}^{N} \sum_{j=1}^{N} \left.\frac{\partial \{\lambda\}}{\partial \alpha_i}\right|_{\alpha=0} [C] \left.\frac{\partial \{\lambda\}^T}{\partial \alpha_j}\right|_{\alpha=0} \quad (55)$$

Where $[C]$ can be written as

$$[C] = \begin{bmatrix} \sigma_{\alpha_1}^2 & cov(\alpha_1, \alpha_2) & \dots & cov(\alpha_1, \alpha_i) \\ cov(\alpha_2, \alpha_1) & \sigma_{\alpha_2}^2 & \dots & cov(\alpha_2, \alpha_i) \\ \dots & \dots & \dots & \dots \\ cov(\alpha_i, \alpha_1) & cov(\alpha_i, \alpha_2) & \dots & \sigma_{\alpha_i}^2 \end{bmatrix}$$
$$(56)$$

Where σ_{α_i} is the standard deviation of random input variables and defined as

$$\sigma_{\alpha_i} = \mu_{\alpha_i} Var\,(\alpha_i) \tag{57}$$

Where μ_{α_i} is the mean values of input random variables and $Var\,(\alpha_i)$ is the variance of random variables from their mean values. Here, $Cov(\alpha_i,\,\alpha_j)$ is a covariance between random variables and zero for statistically independent (i.e., uncorrelated) random variables.

In the second order perturbation method (SOPT), the mean and corresponding variance of response $\{\lambda\}$ can be written as (Shankaran and Mahadevan)

$$\langle\{\lambda\}\rangle = \{\lambda_0\} + \frac{1}{2} Var^I\,[\lambda, \lambda] \tag{58}$$

$$Var^{II}\,[\lambda, \lambda] = Var^I\,[\lambda, \lambda] \tag{59}$$

The coefficient of variance (COV) of response is obtained by the ratio of standard deviation to mean of the response. While, standard deviation can be obtained by square root of variance.

5 Numerical Results and Discussion

In the present study, A MATLAB code in developed for the prediction of statistics of critical buckling temperature of elastically supported piezoelectric laminated composite plate using stochastic finite element method based on SOPT. The lamina material and geometrical properties of plate and piezoelectric at microlevel, foundation parameters, thermal expansion coefficients, volume fraction of fiber are modeled as basic input random variables. The results have been compared with MCS and those available in the literature. A nine-noded Lagrange isoparametric finite element, with 63 degrees of freedom (DOFs) per element for present HSDT model has been used for discretizing the laminate.

The present results are computed by employing the (3x3) integration rule for thick plates and reduced (2x2) rule for thin plates. The mean and COV of critical buckling temperature are obtained by considering all randomness in system properties equal to 20% from their mean values, keeping in mind the limitation of SOPT.

The basic random variables such as V_f, E_{f1}, E_{f2}, E_m, G_{f12}, v_{f12}, h, θ, k_1, k_2, α_1, E_{2p}, G_{12p}, v_{12p}, α_{1p}, and α_{2p} are sequenced and defined as $b_1 = V_f$, $b_2 = E_{f1}$, $b_3 = E_{f2}$, $b_4 = E_m$, $b_5 = G_{f12}$, $b_6 = v_{f12}$, $b_7 = h$, $b_8 = \theta$, $b_9 = k_1$, $b_{10} = k_2$, $b_{11} = \alpha_1$, $b_{12} = E_{2p}$, $b_{13} = G_{12p}$, $b_{14} = v_{12p}$, $b_{15} = \alpha_{1p}$, and $b_{16} = \alpha_{2p}$.

The following dimensionless buckling temperature has been used in this study.

$$\lambda_{Tcr} = \lambda T \alpha_0 \times 10^3$$

Where, λ_{cr}, α_0 and T are the critical buckling temperature, initial thermal expansion coefficients and initial guess temperature, respectively.

For the computational present results, the following properties of composite material at micro level are considered to be temperature dependent on temperature. The material properties taken in analysis are at reference temperature 21 °C and moisture concentration at 0% are given as [27] E_{f1} =220.0 GPa, E_{f2} =13.79 GPa, E_m =3.45 GPa, G_{f1} =8.79 GPa, v_{f12} =0.2, v_m =0.35, $\alpha_{f1} = 0.99\times10^{-6\circ}$/C, $\alpha_{f2} = -10.08\times10^{-6\circ}$/C, α_m =72.0×10$^{-6\circ}$/C, T_{g0} =216°C.

The piezoelectric (5A) material layered at different positions of fiber layers are given as: $E_{11p} = 63.0$ GPa, $E_{22p} = 63.0$ GPa, $G_{12p} = G_{13p} = G_{23p} = 24.3$ GPa, $v_{12p} = 0.3$, $E_{11p} = 63$ GPa,

It is to noted that all the results are shown for linear case except Fig. 11. It is also noted that effect of random system properties $\{b_i = (1,\dots,7) = 0.10\}$, i.e., 10% percentage variation from their mean values are considered (unless otherwise stated). All the random variables are assumed as uncorrelated. The length (a) and width (b) of the plate is considered as unity. The plate geometry used for computation are characterized by namely, plate thickness ratio (a/h), plate aspect ratios, piezoelectric layer (P), fiber volume fraction (V_f), lamination angle (θ) and foundation parameters (k_1) and (k_2) with various numerical value. It is assumed that the uniform variation in temperature change through thickness have been used for computation of results. It is also assumed that two types of foundation parameters have been taken in the present study, namely, I. as Winkler foundation with $(k_1 = 100$, and $k_2 = 0)$ and II. as Pasternak foundation with $(k_1 = 100$, and $k_2 = 10)$ for parametric study, unless status otherwise.

The following boundary conditions are used for computation of results which are given as:

1. **All edges are simply supported (SSSS):**

$$u = w = \theta_y = \psi_y = 0, \text{ at } x = 0, a$$
$$v = w = \theta_x = \psi_x = 0, \text{ at } y = 0, b$$

2. **All edges are Clamped (CCCC):**

$$v = w = \theta_y = \theta_x = \psi_y = \psi_x = 0, \text{ at } x = 0, a$$
$$u = w = \theta_y = \theta_x = \psi_y = \psi_x = 0, \text{ at } y = 0, b$$

3. **Two opposite edge are clamped and others two are simply supported (CSCS):**

$$u = v = w = \theta_y = \theta_x = \psi_y = \psi_x = 0, \text{ at } x = 0$$
$$\text{and } y = 0 \text{ } v = w = \theta_y = \psi_y = 0, \text{ at } x = a;$$
$$u = w = \theta_x = \psi_x = 0, \text{ at } y = 0, \text{ } b$$

5.1 Convergence and validation study

The convergence study of mean buckling temperature of simply supported square laminated $[(45/-45)_3]_S$ composite plate for a/h=10, and V=0.6 is examined by using 3 x 3, 4 x 4, 5 x 5 and 6 x 6 mesh size of elements and plotted in Fig. 2. As the number of mesh size increases, the mean buckling temperature decreases converges from 5 x 5 mesh size. Therefore, the total number of element equal to 25 is taken into consideration for the computation of further numerical results.
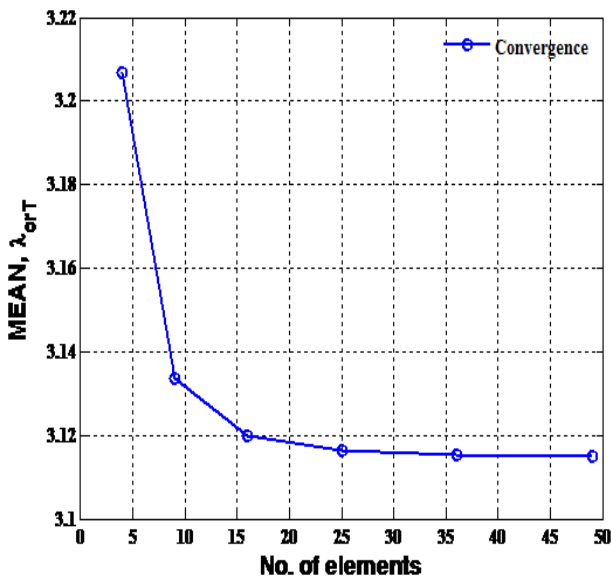
Figure 2: Convergence study for mean buckling temperature of a square laminated composite plate.

The comparison study for mean buckling temperature of angle-ply laminated $[(45/-45)_3]_S$ square composite plate subjected to uniform temperature is shown in Fig. 3. The present results using C^O finite element method are in good agreement with available literature of Shen et al [2010] using semi analytical approach.

The comparison study for different foundation parameters on the thermal buckling of simply supported antisymmetric angle ply plate supported with two parameters
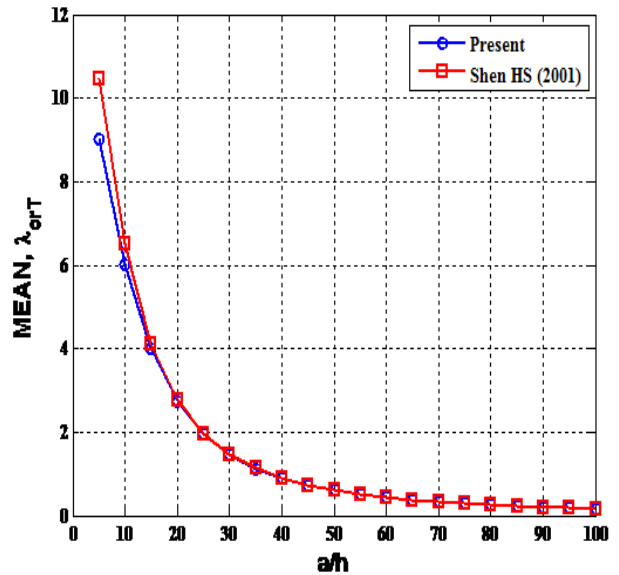
Figure 3: Comparison study for mean buckling temperature of angle-ply laminated $[(45/-45)_3]_S$ square composite plate subjected to uniform temperature.

Pasternak foundation subjected to uniform in-plane temperature is shown in Table 1. The present results using C^O FEM are compared with Chebishev based polynomial results of Pandey et al. [27]. A good agreement with percentage difference of 10% for different value of foundation parameters are achieved between the both results. As the foundation parameters increases, the buckling temperature increases. It is because of foundation parameters increases the stiffness of the plate.

Table 1: Comparison for effect of foundation parameters on the thermal buckling response of [45/-45/45/-45/45/-45] square elastically supported plate subjected to uniform in-plane temperature with TID material properties with a/h=10.

Foundation parameters	Pandey et al. (2010)	Present
200,10	12.3	11.10
100,10	10.7	10.683
50.10	9.95	10.45
0.0	6.02	6.95
50.50	22.5	22.89
50.30	16.24	16.77
50.20	13.10	13.63

Due to unavailability of probabilistic results of present case, the present SOPT results based on perturbation methods are compared with MCS using sampling based

results for thermal buckling of clamped supported laminated $[(45/-45)_3]_S$ square composite plate for a/h=10, V=0.6. The random material properties, b_i (i =1 to7) = 0.10 are assumed as input random variables. For the MCS, the samples value of random system parameters are generated using MATLAB software by assuming normal Gaussian random variables. The samples values are then substituted in response Eq. 47 and generate again a set of samples of response. For the MCS approach 10,000 samples value are sufficient to simulate the results of desired mean and COV of buckling temperature on satisfactory convergence of result. The mean of a set of samples of response will be the mean value of buckling temperature, whereas, SD of samples will be standard deviation (SD) of buckling temperature. The ratio of SD to mean of buckling temperature is defined as COV of buckling temperature. The validation study of mean and COV of buckling temperature of laminated $[(45/-45)_3]_S$ square clamped laminated composite plate for V=0.6 by varying different a/h ratios using SOPT and MCS are examined and shown in Fig. 4(a) and (b). It is observed that both results are in good agreement in terms of mean and COV. It is to be noted that due to very high computational cost, The MCS approach is used for validation purpose only. Although stochastic finite element method based on SOPT relies on low order of polynomial. As the coefficient of variation becomes large, this method becomes inaccurate. Keeping in mind the limitation of SOPT, the COV in random system properties are taken up to 20% (Kleber and Hien 2001).

5.2 Parametric study

The effect of individual random system parameters $\{b_i$ =(1,...,18) =0.10\}$ and fiber volume fraction on the dimensionless mean and COV of critical temperature temperature of piezoelectric elastically supported laminated [P/45/−45/45/−45/45/−45] square plate using SOPT for a/h=10 is shown in Table 2. The effect of COV on buckling temperature with random change in voume fraction of fiber, Young's modulus of fiber and matrix, plate thickness and lamination angle are very high. Therefore, it is concluded that for sensitive and safe applications like aerospace, nuclear and other related applications, tight control of these random system properties are required if high reliability of the plate is desired.

The effect of support conditions (SSSS, CCCC and CSCS) and plate thickness ratios with random change in system parameres $\{b_i$ =(1,..., 7) =0.10\}$ on the mean and COV of buckling temperature of square laminate $[(45/-45)_3]_S$ plate for V_f =0.5 is shown in Fig. 5(a)-(b).
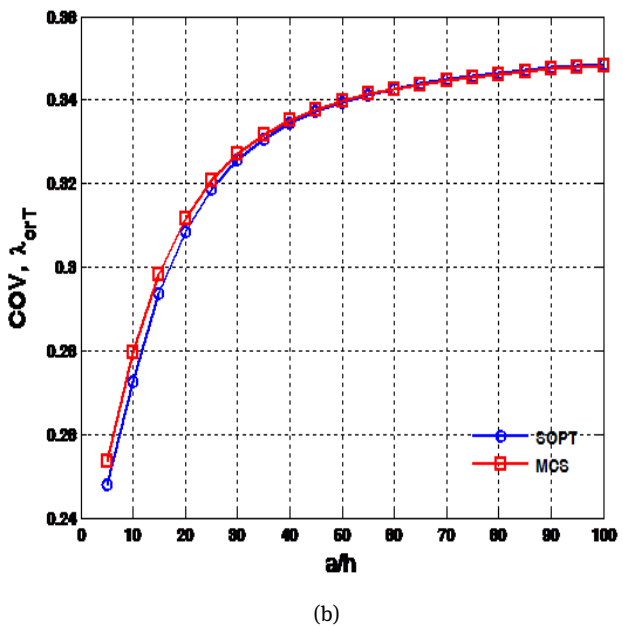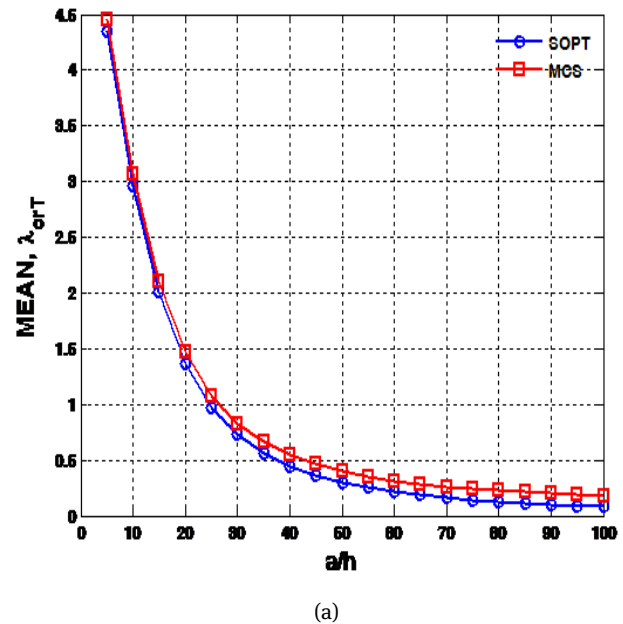

(a)

(b)

Figure 4: The validation study of mean and COV of buckling temperature of laminated square clamped laminated composite plate by varying different a/h ratios using SOPT and MCS.

Among the different support conditions, mean buckling temperature of clamped supported plate is highest while, COV of simply supported plate is highest. It is because of higher boundary constraits increses the mean and decreses the COV of buckling temperature. The change in mean and corresponding COV of buckling temperature for a/h equal to 15 to 45 are highest.

Table 2: Effects of individual random variable and fiber volume fraction on the dimensionless mean and COV of buckling temperature of laminated clamped supported square elastically supported plate.

b_i	Vf=0.4		Vf=0.5		Vf=0.6	
	MEAN	COV	MEAN	COV	MEAN	COV
V_f	2.3029	0.0745	2.7692	0.0879	3.4928	0.1090
E_{f1}	2.3058	0.0489	2.7715	0.0476	3.4846	0.0451
E_{f2}	2.2986	0.0053	2.7621	0.0072	3.4713	0.0096
E_m	2.3097	0.0468	2.7758	0.0433	3.4882	0.0385
G_{f12}	2.3016	0.0097	2.7671	0.0138	3.4800	0.0187
v_{f12}	2.2994	5.5671e-04	2.7633	0.0011	3.4729	0.0019
h	2.3041	0.0800	2.7731	0.0789	3.4940	0.0794
θ	2.5684	0.0747	3.1211	0.0818	3.9643	0.0884
$k_1(100)$	2.3754	0.0031	2.8557	0.0032	3.5879	0.0031
$k_2(10)$	2.7956	0.0176	3.3686	0.0178	4.2254	0.0177
α_1	2.2994	0.0074	2.7634	0.0092	3.4733	0.0116
α_2	2.2994	0.0071	2.7634	0.0107	3.4735	0.0158
E_{1p}	2.2994	0.0015	2.7633	0.0015	3.4729	0.0016
E_{2p}	2.2994	9.3219e-04	2.7633	9.2873e-04	3.4729	9.7068e-04
G_{12p}	2.2994	9.3569e-05	2.7633	9.3569e-05	3.4729	9.3456e-05
v_{12p}	2.2995	0.0010	2.7634	0.0010	3.4731	0.0011
α_{1p}	2.2994	0.0012	2.7633	0.0012	3.4729	0.0013
α_{2p}	2.2994	0.0012	2.7633	0.0012	3.4729	0.0013

The effect of cross-ply and angle-ply symmetric and anti symmetric lamination scheme and plate thickness ratios with random change in system parameres $\{b_i = (1,\ldots,7) = 0.10\}$ on the mean and COV of buckling temperature of square laminated simply supported plate for and $V_f = 0.5$, is shown in Fig. 6(a)-(b). Among the different lamination scheme, mean buckling temperature of antisymmetric cross-ply and agle-ply plate is higher than symmetric cross-ply or angle-ply plate while, COV on buckling temperature of symmetric angle plate is highest. Significant change occures in mean buckling temperature for thick plate while, for COV og buckling temeprature occures for thin plate.

The effect of position of piezoelectric layer at various position of fiber layers and plate thickness ratios with random change in system parameres $\{b_i = (1,\ldots,7) = 0.10\}$ on the mean and COV of buckling temeprature of clamped square laminated compsite plate for $V_f = 0.6$ is shown in Fig. 7(a)-(b). Among the given pizoelectric layer attached at different location of fiber layers, the mean buckling temperature is highest when piezo layer is attached at second place of fiber layer for thick plate while for thin plate, mean buckling temeperature is highest when piezoelectric layer is attached at bottom of the fiber layers. However, COV of buckling temeprature is highest when piezoelectric layer is

attached at first position of fiber layer, while, lowest when piezolayer attached with forth position.

The effect of foundation parameters and plate thickness ratios with random change in only foundation parameres $\{b_i = (9, 10) = 0.10\}$ on the mean and COV of buckling temperature of square clamped laminated [0/90/90/0] square palte for $V_f = 0.6$ is shown in Fig. 8 (a)-(b). As the foundation parameter increses, the buckling temeprature increses. It is because of foundation parameters increse the stiffness of the plate. The increse of buckling temeprature is highest for change in shear foundation. The effect of COV of bucking temeprature is still highst for random change in shear foundation only. The effect of mean and COV are more severe in thick plate.

The effect of volume fration of fiber and plate thickness ratios with random change in all system parameres $\{b_i = (1,\ldots,7) = 0.10\}$ on the mean and COV of buckling temperature of clamped square laminated $[(45/-45)_2]_T$ composite plate is shown in Fig. 9(a)-(b). As the fiber volume fraction increses, the mean buckling temperature increses. However, COV of buckling temperature decreses with increase of fiber volume fraction and effect are more pronounced when low volume of fiber with thin plate is considered.
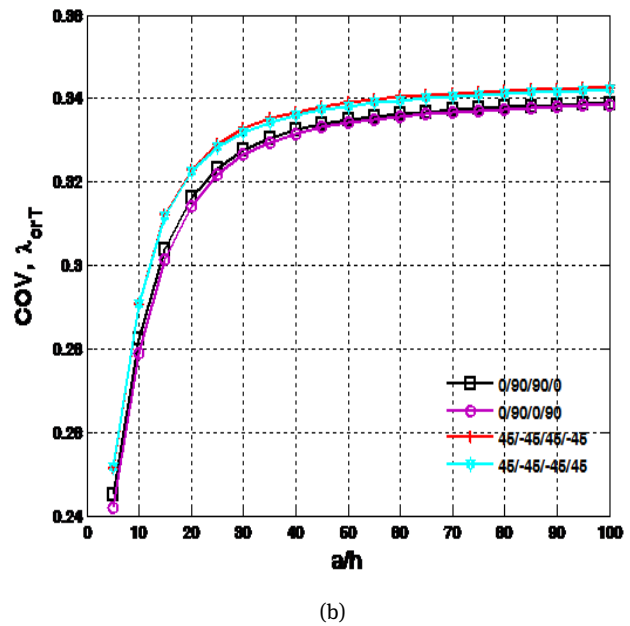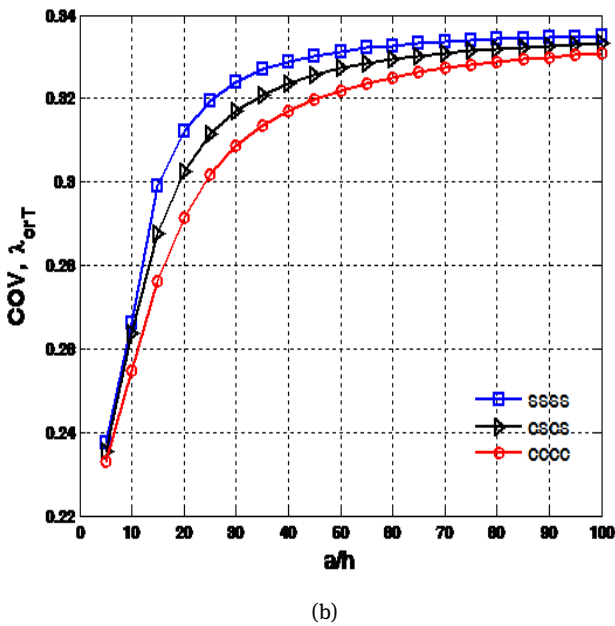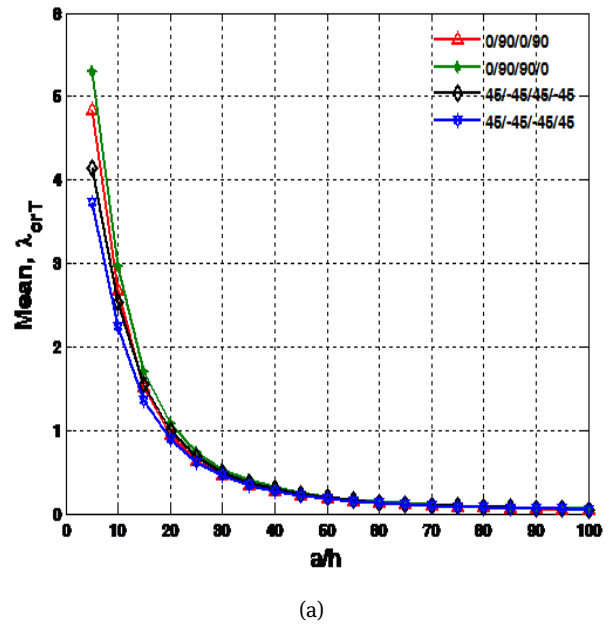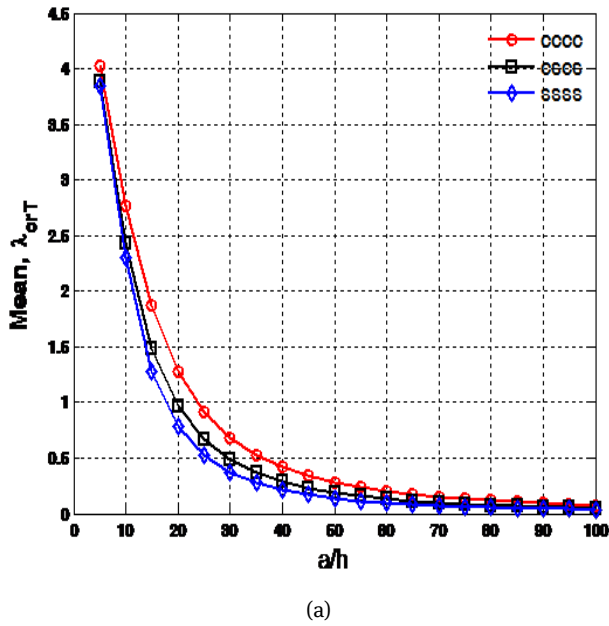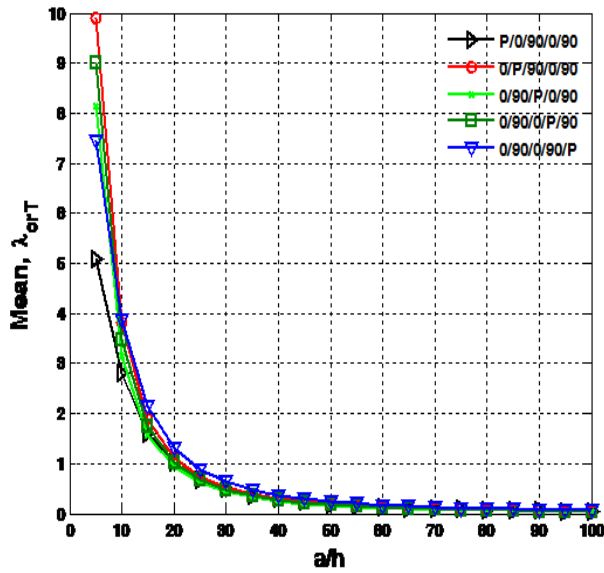
(a)

(b)

Figure 5: Efect of support conditions and plate thickness ratios with random change in all system parameres on the (*a*) mean and (*b*) COV of buckling temperature of square laminate plate.

(a)

(b)

Figure 6: The effect of cross-ply and angle-ply symmetric and anti symmetric lamination scheme and plate thickness ratios with random change in all system parameres on the (a) mean and (b) COV of buckling temeprature.
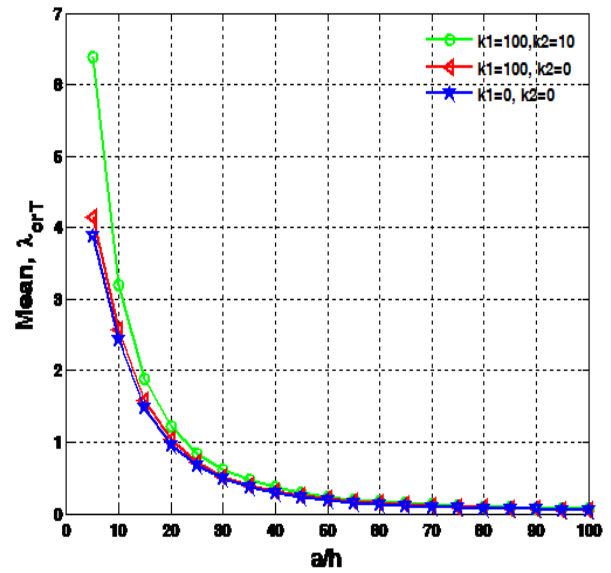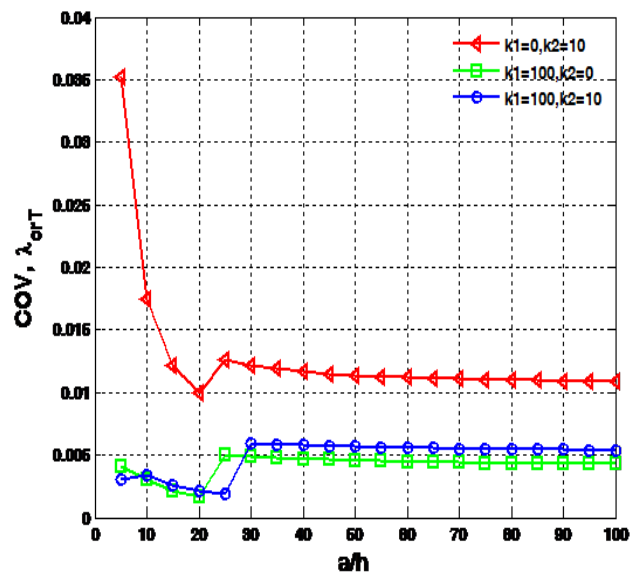
The effect of volume fration of fiber and two layers ply angles $[\theta/\theta]$ with random change in system parameres $\{b_i =(1,\ldots,7) =0.10\}$ on the mean and COV of buckling temperature of simply supported square lamianted compsite plate for a/h=10 is shown in Fig. 10 (a)-(b). As the fiber volume fraction and lamination angle increases, the mean and corresponding COV of buckling temperature in-

creses. The effect of mean buckling temperatue incises up to 45° and then decreses. However, COV of buckling temeprature increases up to 30° and then decrerses and highest at 30°.

The effect of volume fraction of fiber and amlitude ratios with random change in all system parameres

(a)

(a)
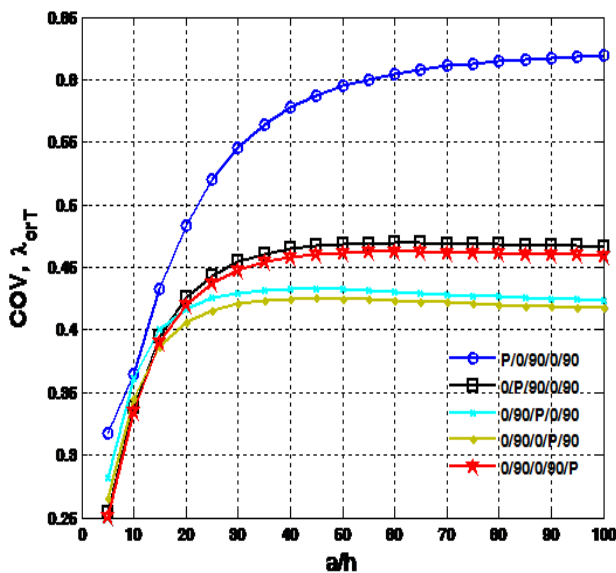
(b)

(b)

Figure 7: Effect of position of piezoelectric layer at various position of fiber layers and plate thickness ratios with random change in all system parameres on mean (a) and (b) COV of buckling temperature.

Figure 8: Effect of foundation parameters and plate thickness ratios with random change in only foundation parameres on the (a) mean and (b) COV of buckling temperature.

$\{b_i = (1,...,7) = 0.10\}$ on the mean and COV of post buckling temperature of clamped square laminated $[(45/-45)_2]_S$ composite plate for $a/h{=}20$ is shown in Fig. 11 (a)-(b). As the amplitude ratio and volume fraction increases, the mean post buckling load increses. While, corresponding COV shows ireguler behavior.
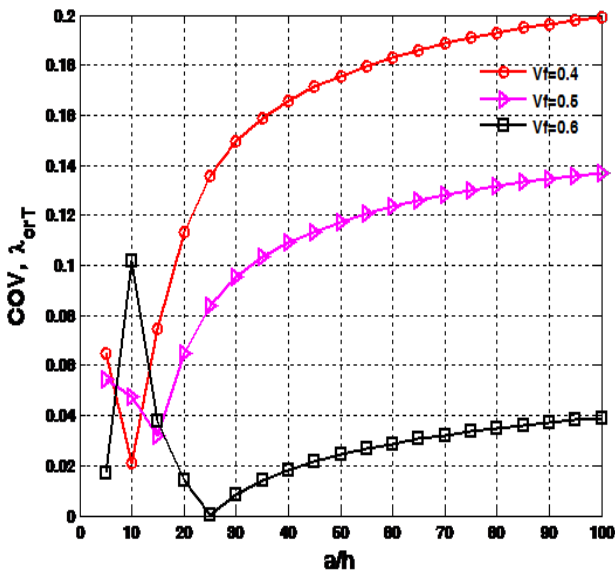
The effect of plate thickness ratio with random change in system parameres $\{b_i = (1,...,7) = 0.05, ...,0.2\}$ on the COV of buckling temperature of clamped square laminated $[(45/-45)_2]_S$ composite plate for $V_f = 0.6$ is shown in Fig. 12 (a)-(b). As the COV of random system properties and plate thickness increses, the COV of mean buckling temperature
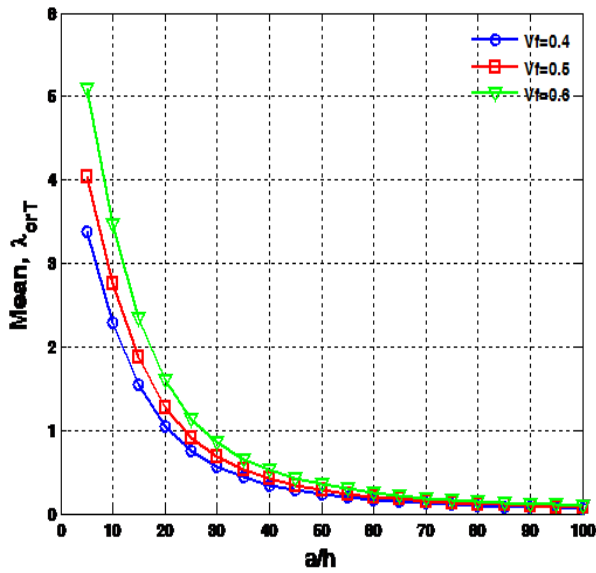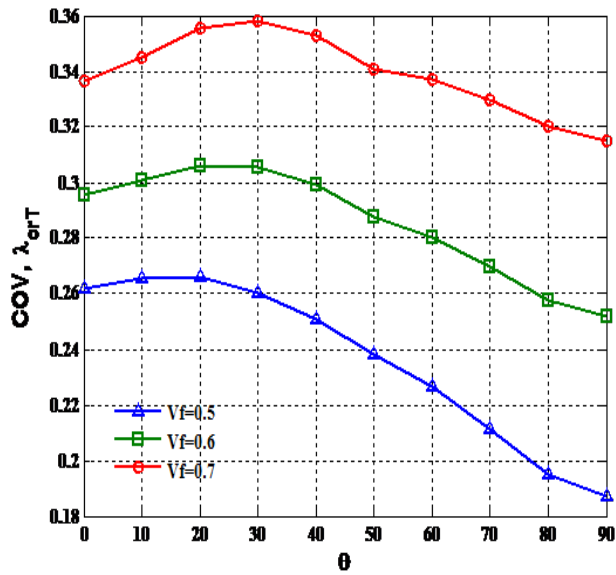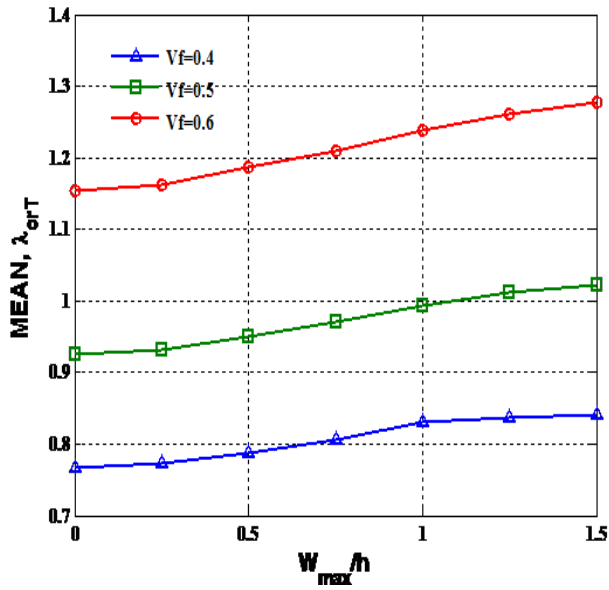
(a)
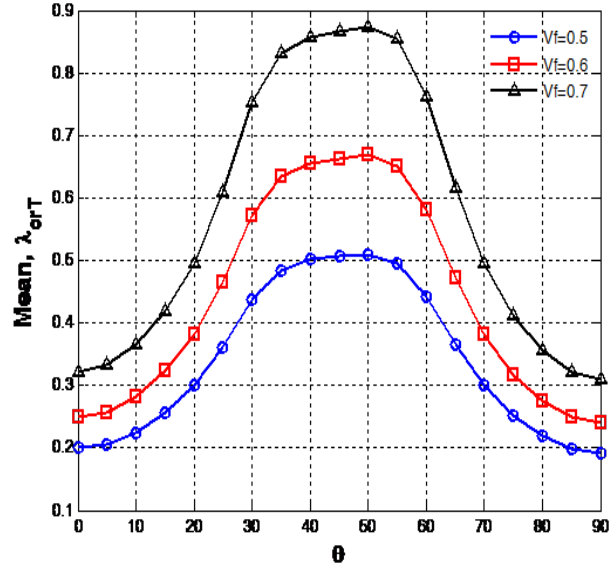
(a)

(b)

(b)

Figure 9: Effect of volume fration of fiber, plate thickness ratios with random change in systemparameres on the (a) mean and (b) COV of buckling temperature.

Figure 10: The effect of volume fration of fiber and two layers ply angles [θ/θ] with random change in system parameres on the (a) mean and (b) COV of buckling temperature.

increses and increment is more severe for higher COV of random system properties with thin plate.

The effect of plate thickness ratio and plate aspect ratios with random change in all system parameres $\{b_i =(1,\dots,7) =0.10\}$ on the mean and COV of buckling temperature of laminated $[(45/-45)_3]_S$ rectangular simply supported composite plate subjected to uni-axial and biaxial

compression for V_f =0.6 is shown in Fig. 13 (a)-(b). As the aspect ratio and plate thickness ratio increses, the mean thermal buckling temeprature increses and corresspond-ing COV decreases. The increses in aspect ratio is more severe as the thickness of the plate dereseases. The mean buckling temperature is higher and corresponding COV is

(a)
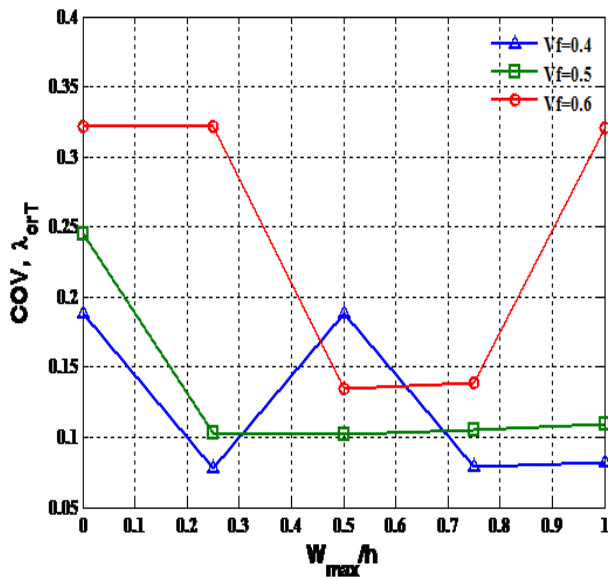
(b)

Figure 11: Effect of volume fraction of fiber and amplitude ratios with random change in system parameres on the mean and COV of thermal post buckling temperature.

lower when the plate is subjected to uniaxial compression as compare to biaxial compression.
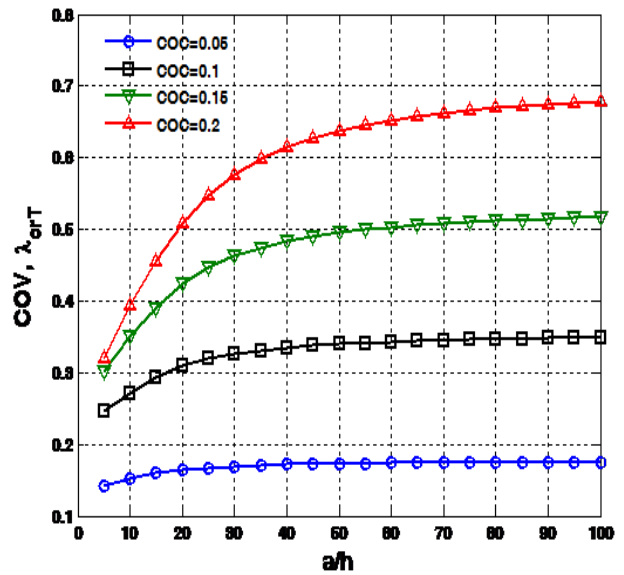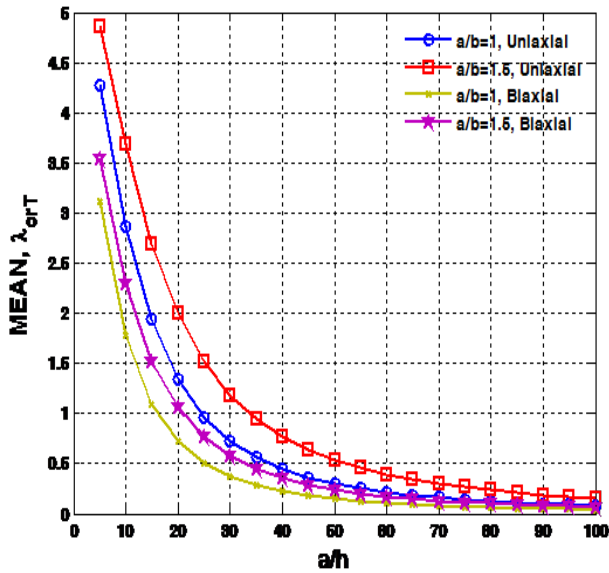

Figure 12: Effect of COV of random change in system properties and plate thickness ratios with random change in system parameters on the COV of buckling temperature.

6 Concluding remarks

A C^0 finite element method based on HSDT with von-Karman nonlinearity in conjunction with SOPT has been presented to obtain the mean and COV of dimensionless buckling temperature of elastically supported piezoelectric laminated composite plate. Form this limited study; the following conclusions can be drawn:

1. The buckling temperature decreases with increase the thickness ratios. The effect is more severe for thick or moderately thick plate.
2. The random change inYoung's modulus of fiber and matrix, plate thickness and lamination angle are very highly sensitive with respect to variation of coeficient of variance. Strict control of these properties are desired for safety point of view.
3. The plate with clamped bundary condition is most desirable for reliability point of view. The effect of support condition is highest for moderaley thick plate
4. The mean of buckling temeprature is higher for antisymmetric cross-ply or angle ply plate while COV is higher for symmetric angle ply plate.
5. The effect of piezoelectric layers attached at top of the fiber layer is highly affeted the variance of thermal buckling temperatures.The proper control of piezolayer at this position is highly required.

(a)
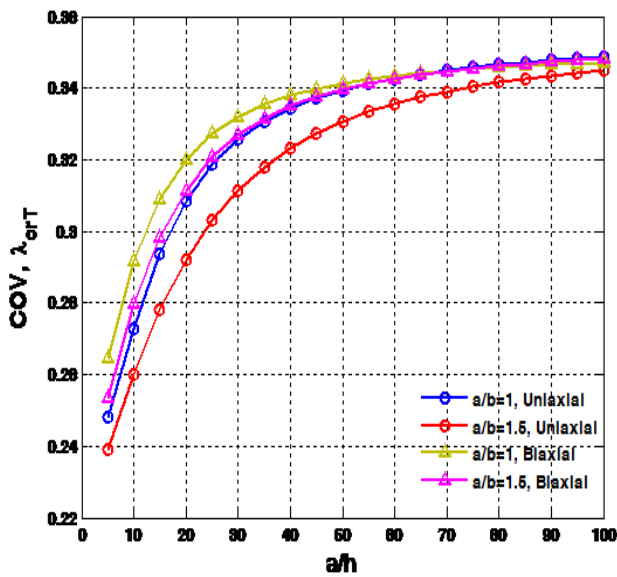
(b)

Figure 13: Effect of plate thickness ratio and plate aspect ratios, with random change in system parameters on the (a) mean and (b) COV of buckling temperature of laminated composite plate subjected to uni-axial and biaxial compression.

6. It is concluded that thick plate resting on elastic foundation shows higher mean buckling temperature and effect of shear forndation is more severe as compared to spring foundation parameters. Therefore, it is concluded that proper caring of shear foun-

dation is required for safety of the elastically supported thick plate.

7. Increment of volime fraction of fiber, increses the mean and decreses the COV of buckling tememprature of the plate. Therefore high volume fraction of thick plate is considered for safety of the structures.

8. Increment of volime fraction of fiber and lamination angle, increses the mean and corresponding COV of buckling tememprature of the plate. The effect of mean and COV of buckling temperature is highest at 45° and 30°, respectively.

9. Increment of volime fraction of fiber and amplitude ratios, increses the mean buckling tememprature of the plate.

10. Increse the coefficent of variance of random system properties, the COV of buckling temperature increses and effect is more severe at higher COV of random system properties and thin plate.

11. Increment of aspect ratios and plate thickness ratios make the mean buckling tememprature higher and corresponding COV lower. For safety point of view, rectanguler thick plate is more desirable.

Appendix

$$[T] = \begin{bmatrix} 1 & 0 & 0 & z & 0 & 0 & z^3 & 0 & 0 & 0 & 0 & 0 & 0 \\ 0 & 1 & 0 & 0 & z & 0 & 0 & z^3 & 0 & 0 & 0 & 0 & 0 \\ 0 & 0 & 1 & 0 & 0 & z & 0 & 0 & z^3 & 0 & 0 & 0 & 0 \\ 0 & 0 & 0 & 0 & 0 & 0 & 0 & 0 & 0 & 1 & 0 & z^2 & 0 \\ 0 & 0 & 0 & 0 & 0 & 0 & 0 & 0 & 0 & 0 & 1 & 0 & z^2 \end{bmatrix},$$
(A.1)

$$[T_\varphi] = \begin{bmatrix} 1 & 0 & z & 0 & z^2 & 0 & 0 & 0 \\ 0 & 1 & 0 & z & 0 & z^2 & 0 & 0 \\ 0 & 0 & 0 & 0 & 0 & 0 & 1 & z \end{bmatrix}, \quad \text{(A.2)}$$

$$Q = \begin{bmatrix} \bar{Q}_{11} & \bar{Q}_{12} & \bar{Q}_{16} & 0 & 0 \\ \bar{Q}_{12} & \bar{Q}_{22} & \bar{Q}_{26} & 0 & 0 \\ \bar{Q}_{16} & \bar{Q}_{26} & \bar{Q}_{66} & 0 & 0 \\ 0 & 0 & 0 & \bar{Q}_{44} & \bar{Q}_{45} \\ 0 & 0 & 0 & \bar{Q}_{45} & \bar{Q}_{55} \end{bmatrix} \quad \text{(A.3)}$$

$$\bar{Q}_{11} = Q_{11}\cos^4\alpha + 2(Q_{12}+2Q_{66})\cos^2\alpha\sin^2\alpha$$
$$+Q_{22}\sin^4\alpha$$

$$\bar{Q}_{12} = \overline{Q}_{21} = (Q_{11}+Q_{22}-4Q_{66})\cos^2\alpha\sin^2\alpha$$
$$+Q_{12}\left(\cos^4\alpha+\sin^4\alpha\right)$$

$$\bar{Q}_{16} = (Q_{11}-Q_{12}-2Q_{66})\sin\alpha\cos^3\alpha$$
$$+(Q_{12}-Q_{22}+2Q_{66})\sin^3\alpha\cos\alpha$$

$$\bar{Q}_{22} = Q_{11}\sin^4\alpha + 2(Q_{12}+2Q_{66})\cos^2\alpha\sin^2\alpha$$
$$+Q_{22}\cos^4\alpha$$

$$\bar{Q}_{26} = (Q_{11}-Q_{12}-2Q_{66})\sin^3\alpha\cos\alpha$$
$$+(Q_{12}-Q_{22}+2Q_{66})\sin\alpha\cos^3\alpha$$

$$\bar{Q}_{66} = (Q_{11}+Q_{22}-2Q_{12}-2Q_{66})\cos^2\alpha\sin^2\alpha$$
$$+Q_{66}\left(\cos^4\alpha+\sin^4\alpha\right)$$

$$\bar{Q}_{44} = Q_{44}\cos^2\alpha + Q_{55}\sin^2\alpha$$
$$\bar{Q}_{45} = (Q_{55}-Q_{44})\sin\alpha\cos\alpha - Q_{54}$$
$$\bar{Q}_{55} = Q_{55}\cos^2\alpha + Q_{44}\sin^2\alpha$$

with

$$Q_{11}=\frac{E_{11}}{(1-\nu_{12}\nu_{21})}\;,\quad Q_{12}=\frac{\nu_{12}E_{22}}{(1-\nu_{12}\nu_{21})}=\frac{\nu_{21}E_{11}}{(1-\nu_{12}\nu_{21})}=Q_{21}\;,$$
$$Q_{22}=\frac{E_{22}}{(1-\nu_{12}\nu_{21})}\;,\quad Q_{66}=G_{12}\;,\quad Q_{44}=G_{13}\;,\quad Q_{55}=G_{12}\;,$$
$$nu_{21}=\frac{\nu_{12}E_{22}}{E_{11}}$$

$$\varphi(x,y,z)=\varphi^{(0)}(x,y)+z\varphi^{(1)}(x,y)+z^2\varphi^{(2)}(x,y).\quad\text{(A.4)}$$

$$[k]=\begin{bmatrix} k_{11} & k_{12} & 0 \\ k_{12} & k_{22} & 0 \\ 0 & 0 & k_{33} \end{bmatrix}.\quad\text{(A.5)}$$

$$D=\sum_{k=1}^{NL}\int_{z_{k-1}}^{z_k}[T]^T\,[\overline{Q}]\,[T]\,dz$$

$$=\begin{bmatrix} [A_1] & [B] & [E] & 0 & 0 \\ [B] & [C_1] & [F_1] & 0 & 0 \\ [E] & [F_1] & [H] & 0 & 0 \\ 0 & 0 & 0 & [A_2] & [C_2] \\ 0 & 0 & 0 & [C_2] & [F_2] \end{bmatrix}\quad\text{(A.6a)}$$

with

$$\left(A_{1_{ij}},\quad B_{ij},\quad C_{1_{ij}},\quad E_{ij},\quad F_{1_{ij}},\quad H_{ij} \right)$$
$$=\sum_{k=1}^{NL}\int_{z_{k-1}}^{z_k}\overline{Q}_{ij}^{(k)}\left(1,\quad z,\quad z^2,\quad z^3,\quad z^4,\quad z^6 \right)dz,$$

For i,j=1,2,6,

$$\{\overline{\varepsilon_L}\}=[L]\{\Lambda\},$$

For i,j=4,5,

$$[D_1]=\sum_{k=1}^{NL}\int_{z_{k-1}}^{z_k}[T]^T\,[e]\,[T]\,dz$$

$$=\begin{bmatrix} [0] & [0] & [0] & [M_1] & [N_1] \\ [0] & [0] & [0] & [N_1] & [P_1] \\ [0] & [0] & [0] & [Q_1] & [R_1] \\ [M_2] & [N_2] & [P_2] & [0] & [0] \\ [P_2] & [Q_2] & [R_2] & [0] & [0] \end{bmatrix},\quad\text{(A.6b)}$$

with $\left(M_{1_{ij}},\quad N_{1_{ij}},\quad P_{1_{ij}},\quad Q_{1_{ij}},\quad R_{1_{ij}} \right)$

$$=\sum_{k=1}^{NL}\int_{z_{k-1}}^{z_k}e_{ij}^{(k)}\left(1,\quad z,\quad z^2,\quad z^3,\quad z^4 \right)dz,$$

where i=3, j=1,2,6,

$$\left(M_{2_{ij}},\quad N_{2_{ij}},\quad P_{2_{ij}},\quad Q_{2_{ij}},\quad R_{2_{ij}} \right)$$

$$=\sum_{k=1}^{NL}\int_{z_{k-1}}^{z_k}e_{ij}^{(k)}\left(1,\quad z,\quad z^2,\quad z^3,\quad z^4 \right)dz,$$

where i=1,2, j=4,5,

$$[D_2]=\sum_{k=1}^{NL}\int_{z_{k-1}}^{z_k}[T_\varphi]^T\,[k]\,[T_\varphi]\,dz$$

$$=\begin{bmatrix} [S_1] & [T_1] & [U_1] & [0] & [0] \\ [T_1] & [U_1] & [V] & [0] & [0] \\ [U_1] & [V] & [W] & [0] & [0] \\ [0] & [0] & [0] & [S_2] & [T_2] \\ [0] & [0] & [0] & [T_2] & [U_2] \end{bmatrix},\quad\text{(A.6c)}$$

with

$$\left(S_{1_{ij}},\quad T_{1_{ij}},\quad U_{1_{ij}},\quad V_{ij},\quad W_{ij} \right)$$

$$=\sum_{k=1}^{NL}\int_{z_{k-1}}^{z_k}k_{ij}^{(k)}\left(1,\quad z,\quad z^2,\quad z^3,\quad z^4 \right)dz,$$

where i,j=1,2,

$$\left(S_{2_{ij}},\quad T_{2_{ij}},\quad U_{2_{ij}} \right)=\sum_{k=1}^{NL}\int_{z_{k-1}}^{z_k}k_{ij}^{(k)}\left(1,\quad z,\quad z^2 \right)dz,$$

$$D_3 = \begin{bmatrix} A_1 & 0 \\ B & 0 \\ E & 0 \\ 0 & A_2 \\ 0 & C_2 \end{bmatrix}, \text{ where i,j=3.}$$

$$D_5 = \begin{bmatrix} A_1 & 0 \\ 0 & A_2 \end{bmatrix}, D_4 = \begin{bmatrix} A_1 & B & E & 0 & 0 \\ 0 & 0 & 0 & A_2 & C_2 \end{bmatrix},$$

$$D_6 = \begin{bmatrix} 0 & 0 & 0 & M_1 & N_1 \\ M_2 & N_2 & P_2 & 0 & 0 \end{bmatrix}, D_7 = \begin{bmatrix} 0 & M_2 \\ 0 & N_2 \\ 0 & P_2 \\ M_1 & 0 \\ N_1 & 0 \end{bmatrix},$$

$$(A.7)$$

$$\bar{N}_0^T = \begin{bmatrix} N_x^T & M_x^T & M_x^T \\ N_y^T & M_y^T & M_y^T \\ N_{xy}^T & M_{xy}^T & M_{xy}^T \end{bmatrix} \qquad (A.8)$$

$$= \sum_{k=1}^{NL} \int_{z_{k-1}}^{z_k} \begin{bmatrix} A_x \\ A_y \\ A_{xy} \end{bmatrix} \left(1, z, z^2\right) \Delta T dz \qquad (A.9)$$

where

$$\begin{bmatrix} A_x \\ A_y \\ A_{xy} \end{bmatrix} = - \begin{bmatrix} \overline{Q_{11}} & \overline{Q_{12}} & \overline{Q_{16}} \\ \overline{Q_{12}} & \overline{Q_{22}} & \overline{Q_{26}} \\ \overline{Q_{16}} & \overline{Q_{26}} & \overline{Q_{66}} \end{bmatrix} \begin{bmatrix} c^2 & s^2 \\ s^2 & c^2 \\ 2cs & -2cs \end{bmatrix} \begin{bmatrix} \alpha_{11} \\ \alpha_{22} \\ \alpha_{12} \end{bmatrix}$$

References

[1] Prabhu M.R., Dhanaraj R., Thermal buckling of laminated composite plates, Comp. Struct., 1994, 53, 1193-1204.

[2] Chen Lien-wen, Chen Lei-Yi., Thermal buckling behaviour of laminated composite plates with temperature-dependent properties, Compos. Struct., 1989, 13(4), 275–87.

[3] Shen H.S., Thermal post buckling behaviour of imperfect shear deformable laminated plates with temperature-dependent properties, Comput. Meth. Appl. Mech. Eng. 2001, 190, 5377–90.

[4] Srikanth G., Kumar A. Post buckling response and failure of symmetric laminates under uniform temperature rise, Compos. Struct., 2003, 59, 109–18.

[5] Shariyat M., Thermal buckling analysis of rectangular composite plates with temperature-dependent properties based on a layer wise theory, Thin-Walled Struct., 2007, 45(4), 439–52.

[6] Pandey R., Shukla K.K., Jain A., Thermoelastic stability analysis of laminated composite plates, an analytical approach, Commun. Nonl. Sci. Numer. Simulat., 2008, 14(4), 1679–99.

[7] Shukla K.K., Huang J.H., Nath Y., Thermal post buckling of laminated composite plates with temperature dependent properties, J. Engin.Mech., ASCE, 2004, 130(7), 818-825.

[8] Jifeng Xu, Qun Zhao, Pizhong Qiao, A Critical Review on Buckling and Post-Buckling Analysis of Composite Structures, Fron. Aero. Eng., 2013, 2(3), 157-168.

[9] Fatima Zohra Kettaf, Mohammed Sid Ahmed Houari, Mohamed Benguediab, Abdelouahed Tounsi, Thermal buckling of functionally graded sandwich plates using a new hyperbolic shear displacement model, Steel and Compos. Struct., 2013,15(4), 399-423.

[10] Grover N., Singh B. N., Maiti D. K., Free vibration and buckling characteristics of laminated composite and sandwich plates implementing a secant function based shear deformation theory, Proceed. Instit. Mech. Eng., Part C: J. Mech. Eng. Sc, 2015, 229(3), 391-405.

[11] Patel B.P., Ganapati M., Prasad K.R., Makhecha D.P., Dynamic stability of layered anisotropic composite plates resting on elastic foundation, Eng. Struct., 1999, 35, 345-355.

[12] Shen H.S., Zheng J.J., Huang X.L., Dynamic response of shear deformable plates under thermomechancial loadings, and resting on elastic foundation. Compos. Struct., 2003,60, 57-66.

[13] Setoodes A.R., Karmi G., Static, free vibration and buckling analysis of anisotropic thick laminated composite plates on distributed and point elastic supports using 3-D layer wise FEM, Eng. Struct., 2004, 26, 211-220.

[14] Jayachandran S.A., Vaidynathan C.V., Post critical behavior of biaxial compressed plate on elastic foundations, Comput. Struct., 1995,54(2), 239-246.

[15] Shen H.S., Williams F.W., Biaxial buckling and post buckling of composite laminated plates on two parameters elastic foundations, Comput. Struct., 1997, 63(6), 1177-1185.

[16] Shen H.S., Post buckling of shear deformable laminated plates under biaxial compression and lateral pressure and resting on elastic foundation, Int. J. Mech. Scien., 2000, 42 (6), 1171-1195.

[17] Shen H.S., Post buckling analysis of composite plates on two parameters elastic foundation, Int. J. Mech. Scien., 1995, 37 (12), 1307-1316.

[18] Xia X.K., Shen H.S., Nonlinear vibration and dynamic response of FGM plates with piezoelectric fiber reinforced composite actuators, Compos. Struct., 2009, 90, 254–262.

[19] Shen H.S., A comparison of buckling and post buckling behavior of FGM plates with piezoelectric fiber reinforced composite actuators, Compos. Struct., 2009, 91, 375–384.

[20] Shen H., Zheng Hong Zhu, Compressive and thermal post buckling behaviors of laminated plates with piezoelectric fiber reinforced composite actuators, Appli. Math. Model., 2011, 35(4), 1829–1845.

[21] Naveen C., Singh B. N., Thermal buckling and post-buckling of laminated composite plates with sma fibers using layerwise theory. Int. J. Comput.l Meth. Engin. Sci. Mechan, 2009.10 (6), 423-429

[22] Panda S. K., Singh B. N., Thermal Post-buckling behaviour of laminated composite cylindrical/hyperboloid shallow shell panel using nonlinear finite element method by Compos. Struct., 2009,91(3), 366-374.

[23] Chamis C.C., Simplified composite micromechanics equations for mechanical, thermal and moisture related properties. Engin. Guide to comp. mater. ASM Int., Materials Park, Ohio, 1987, 3.8–3.24.

[24] Chamis C.C., Sinclair J.H., Durability/life of fiber composites in hygrothermomechanical environments. Composite Materials: Testing and Design (Sixth Conf.) STP 787, ASTM, West Conshohocken, Pa., 1982, 498–512.

[25] Chandra R., Singh S.P., Gupta K., Micromechanical damping models for fiber-reinforced composites: A comparative study.

Composites, 2002, Part A. 33, 787–796.

[26] Chao L.P., Shyu S.L., Nonlinear buckling of fiber reinforced composite plates under hygrothermal effects. J. Chinese Inst. Eng. 1996, 19, 657–667.

[27] Pandey R., Upadhyay A.K., Shukla K.K., Hygrothermoelastic post buckling response of laminated composite plates, J. Aeros. Engg., ASCE, 2010, 23(1), 1-13.

[28] Graham L.L., Siragy E.F., Stochastic finite element for elastic buckling of stiffened panels, ASCE J Eng. Mech., 2001, 127(1), 91-97.

[29] Onkar A.K., Upadhyay C.S., Yadav D., Stochastic finite element analysis buckling analysis of laminated with circular cutouts under uniaxial compression. Trans ASME J Appl. Mech. 2007, 74, 789–809.

[30] Verma V.K., Singh B.N., Thermal buckling of laminated composite plates with random geometric and material properties, Int. J.Struct. Stab. Dynam., 9(2), 2009, 187-211.

[31] Lal A., Singh B. N., Thermal buckling response of laminated composite plate with random system properties, Int. J. Comput. Meth. 2009, 6(2), 447-471.

[32] Lal A., Singh B.N., Kumar R., Effects of random system properties on the thermal buckling analysis of laminated composite plates, Comput. Struct., 2009, 87 (17-18), 1119.

[33] Singh B. N., Jibumon B., Thermal buckling of conical panel/shell embedded with and without piezoelectric layers with random material properties. Int. J. Crashworthiness, 2009, 14(1), 73-81.

[34] Kumar R., Patil H.S., Lal A., Hygrothermoelastic buckling response of laminated composite plates with random system properties: macromechanical and micromechanical model, J. Aerosp. Eng., 2012, 10.1061/(ASCE)AS.1943-5525.0000241, 04014123.

[35] Reddy J. N., A simple higher-order theory for laminated composite plates, J. Appl. Mech. 1984, 51, 745-752.

[36] Kleiber M., Hien T.D., The stochastic finite element method, John Wiley and Sons, 1992.

[37] Haldar A., Mahadevan S., Reliability assessment using stochastic finite element analysis. John Willey and Sons, 2000.

[38] Gibson R. F., Principles of composite material mechanics, McGraw-Hill, 1994.

[39] Jones R. M., Mechanics of composite materials, McGraw-Hill, New York, 1975.